

Supporting Information

Three AIE-ligand-based Cu(I) Coordination Polymers: Synthesis, Structures and Luminescence Sensing TNP

Jinfang Zhang*, Hongchen Xia, Simeng Ren, Wen Jia, Chi Zhang*

*International Joint Research Center for Photoresponsive Molecules and Materials, School of Chemical
and Material Engineering, Jiangnan University, Wuxi 214122, P. R. China*

Table of contents

- 1. Fig. S1** The asymmetric unit of **1**.
- 2. Fig. S2** The asymmetric unit of **2**.
- 3. Fig. S3** ABAB-arranged rhombic channels in **2** viewed along *c* axis.
- 4. Fig. S4** The asymmetric unit of **3**.
- 5. Fig. S5** The windmill-like shape in **3**.
- 6. Fig. S6** The angle between two pyridine rings of bridged DPMF in **1** (a), **2** (b) and **3** (c).
- 7. Fig. S7** The PXRD patterns of **1** (a), **2** (b) and **3** (c).
- 8. Fig. S8** The PXRD patterns of **3** in different situations.
- 9. Fig. S9** The TGA curves of **1-3**.
- 10. Fig. S10** Luminescence quenching spectra of **3** for NB (a), 1,3-DNB (b), 4-NT (c) and 2,4-DNT (d).
- 11. Fig. S11** Stern-Volmer plot for NB (a), 1,3-DNB (b), 4-NT (c) and 2,4-DNT (d) of **3** in DMF suspension at the low concentration.
- 12. Fig. S12** The detection limit for NB (a), 1,3-DNB (b), 4-NT (c) and 2,4-DNT (d) of **3** in DMF.
- 13. Fig. S13** Optical images of test papers with different NACs under 365nm UV light.
- 14. Table S1** Selected bond lengths (\AA) for **1**; **Table S2** Selected angles ($^\circ$) for **1**.
- 15. Table S3** Selected bond lengths (\AA) for **2**; **Table S4** Selected angles ($^\circ$) for **2**.
- 16. Table S5** Selected bond lengths (\AA) for **3**; **Table S6** Selected angles ($^\circ$) for **3**.

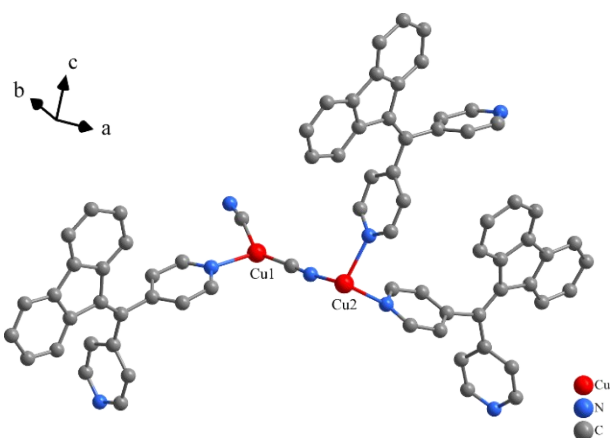


Fig. S1 The asymmetric unit of **1**.

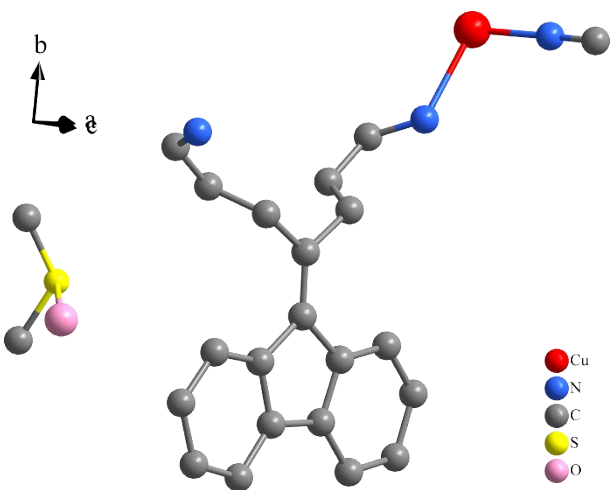


Fig. S2 The asymmetric unit of **2**.

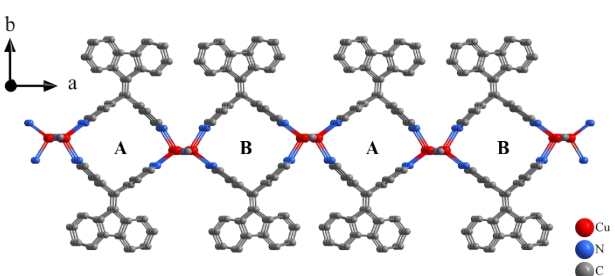


Fig. S3 ABAB-arranged rhombic channels in **2** viewed along *c* axis.

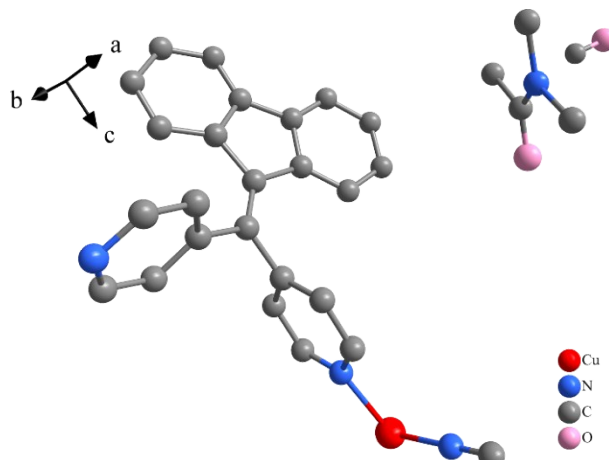


Fig. S4 The asymmetric unit of **3**.

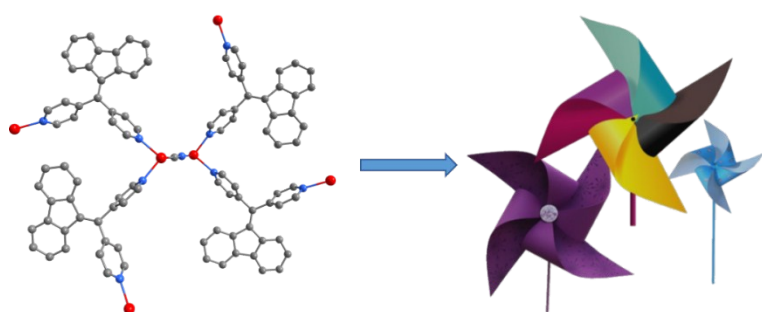


Fig. S5 The windmill-like shape in **3**.

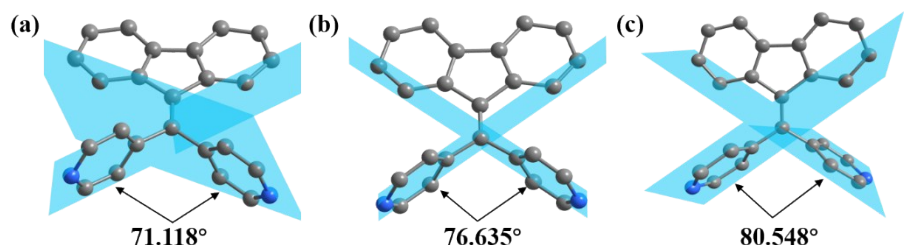


Fig. S6 The angle between two pyridine groups of bridged DPMF in **1** (a), **2** (b) and **3** (c).

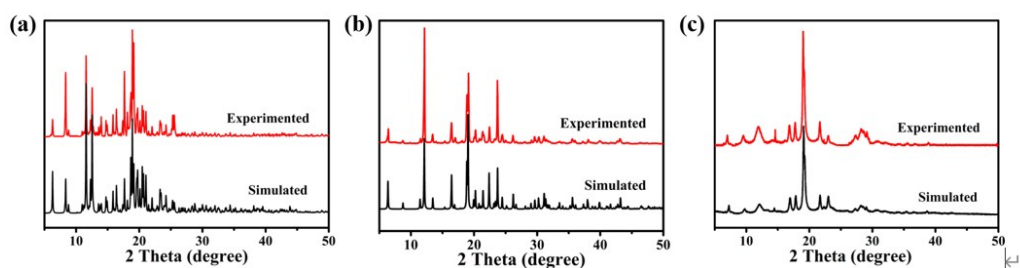


Fig. S7 The PXRD patterns of **1** (a), **2** (b) and **3** (c).

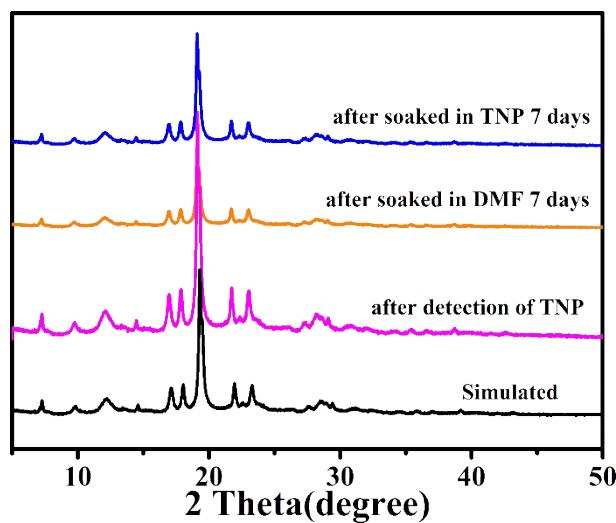


Fig. S8 The PXRD patterns of **3** in different situations.

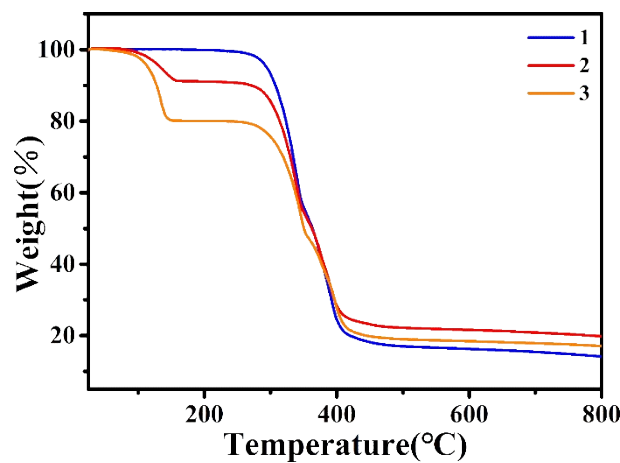


Fig. S9 The TGA curves of **1-3**.

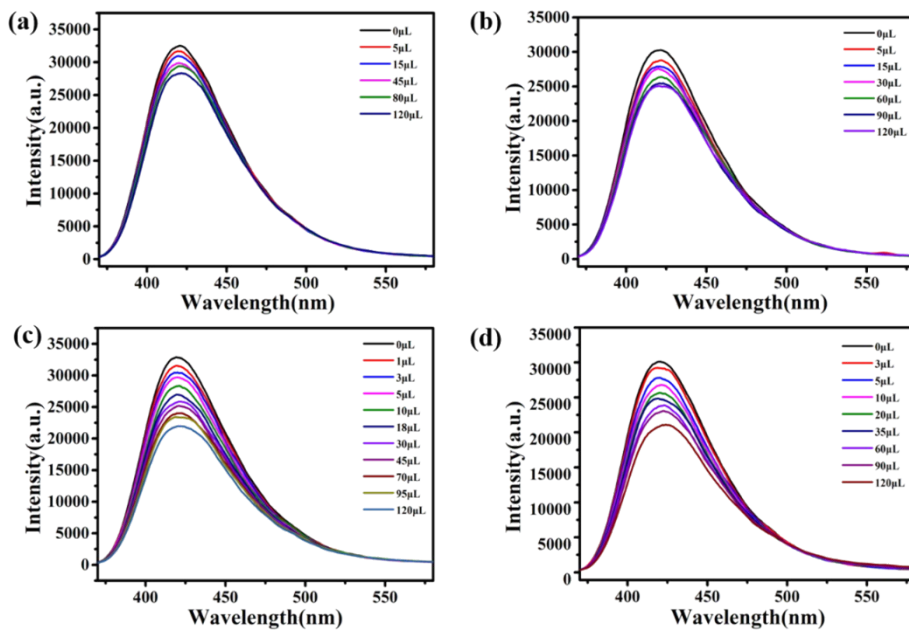


Fig. S10 Luminescence quenching spectra of **3** for NB (a), 1,3-DNB (b), 4-NT (c) and 2,4-DNT (d).

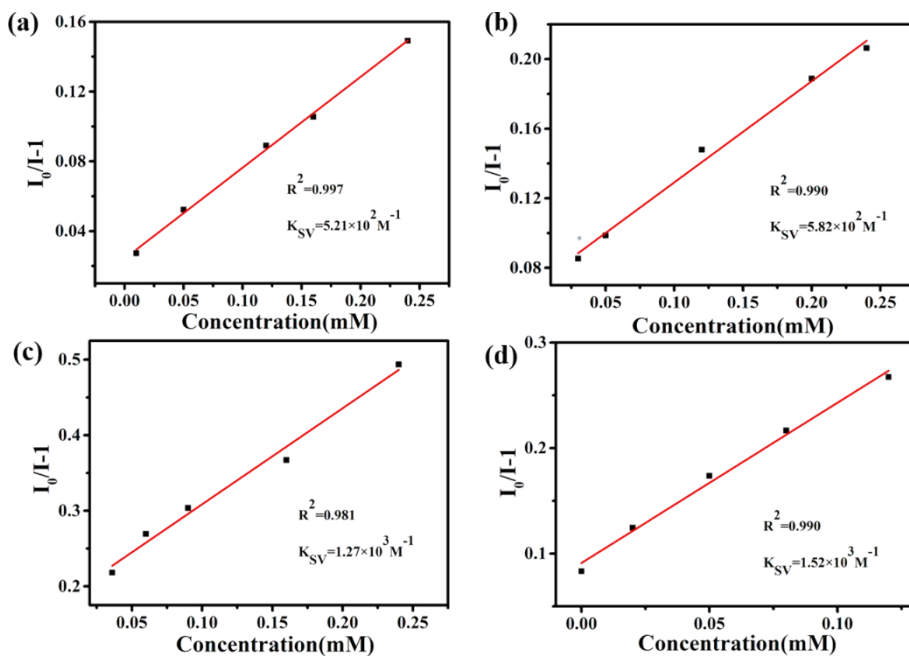


Fig. S11 Stern-Volmer plot for NB (a), 1,3-DNB (b), 4-NT (c) and 2,4-DNT (d) of **3** in DMF suspension at the low concentration.

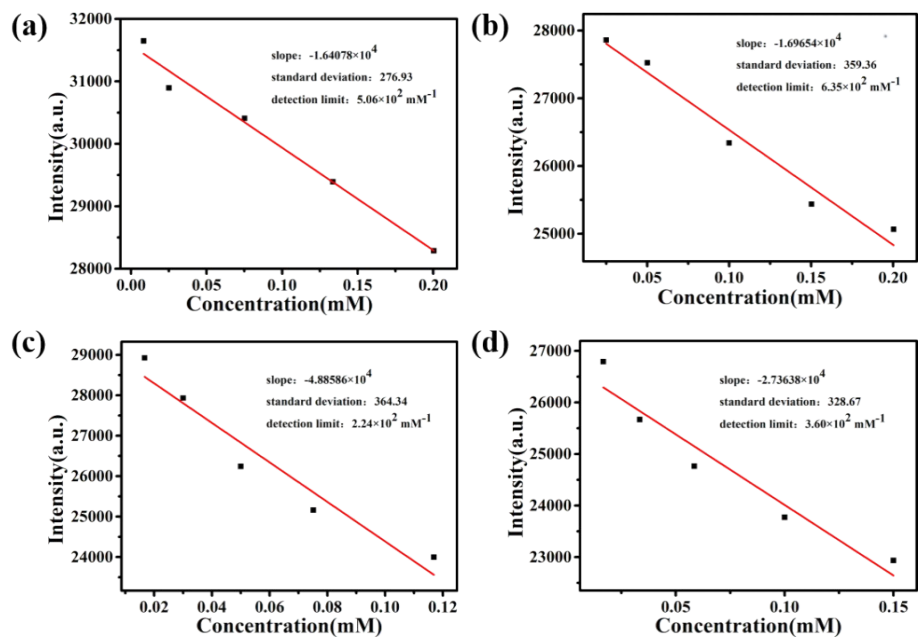


Fig. S12 The detection limit for NB (a), 1,3-DNB (b), 4-NT (c) and 2,4-DNT (d) of **3** in DMF.

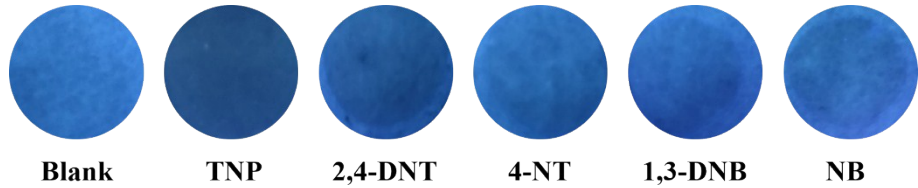


Fig. S13 Optical images of test papers with different NACs under 365nm UV light.

Table S1 Selected bond lengths (\AA) for **1**

1			
Cu(1)-C(72)	1.910(4)	Cu(1)-N(2)	2.166(3)
Cu(1)-N(8)#1	1.929(4)	Cu(1)-N(1)#2	2.311(4)
N(3)-Cu(2)	2.216(4)	N(5)-Cu(2)	2.230(3)
N(7)-Cu(2)	1.925(4)	Cu(2)-C(73)	1.905(4)
#1 -x+1,-y+2,-z+1	#2 x,y-1,z	#3 x,y+1,z	

Table S2 Selected angles ($^{\circ}$) for **1**

1			
C(72)-Cu(1)-N(8)#1	145.44(19)	C(1)-N(1)-Cu(1)#2	119.5(3)
C(72)-Cu(1)-N(2)	105.27(15)	C(5)-N(1)-Cu(1)#2	123.3(3)
N(8)#1-Cu(1)-N(2)	101.46(15)	C(29)-N(3)-Cu(2)	119.6(3)
C(72)-Cu(1)-N(1)#2	106.61(16)	C(25)-N(3)-Cu(2)	123.0(3)
N(8)#1-Cu(1)- N(1)#2	94.92(16)	C(48)-N(5)-Cu(2)	116.5(3)
N(2)-Cu(1)-N(1)#2	89.72(15)	C(52)-N(5)-Cu(2)	125.6(3)
C(73)-N(8)-Cu(1)#3	166.6(4)	C(72)-N(7)-Cu(2)	174.3(4)
C(73)-Cu(2)-N(7)	145.65(18)	C(73)-Cu(2)-N(5)	97.28(16)
C(73)-Cu(2)-N(3)	102.82(16)	N(7)-Cu(2)-N(5)	104.15(15)
N(7)-Cu(2)-N(3)	102.84(15)	N(3)-Cu(2)-N(5)	92.19(15)
N(7)-C(72)-Cu(1)	176.0(4)	N(8)-C(73)-Cu(2)	168.9(4)
C(11)-N(2)-Cu(1)	120.3(3)	C(7)-N(2)-Cu(1)	121.8(3)
#1 -x+1,-y+2,-z+1	#2 x,y-1,z	#3 x,y+1,z	

Table S3 Selected bond lengths (\AA) for **2**

2			
Cu(1)-N(1')	1.846(12)	Cu(1)-N(2)	2.237(7)
Cu(1)-N(3)#1	2.174(6)	Cu(1)-C(1)	2.025(2)
#1 -x+1/2,-y+1/2,-z+1	#2 x,y,-z+1		

Table S4 Selected angles ($^{\circ}$) for **2**

2			
N(1')-Cu(1)-N(3)#1	102.1(4)	C(7)#2-N(2)-Cu(1)	120.9(4)
N(1')-Cu(1)-N(2)	102.9(4)	C(7)-N(2)-Cu(1)	120.9(4)
N(3)#1-Cu(1)-N(2)	95.2(2)	C(1)-N(3)-Cu(1)#1	122.2(3)
C(1')-N(1')-Cu(1)	164.8(12)	C(1)#2-N(3)-Cu(1)#1	122.2(3)
#1 -x+1/2,-y+1/2,-z+1	#2 x,y,-z+1		

Table S5 Selected bond lengths (\AA) for **3**

3			
Cu(1)-C(31)	1.885(5)	Cu(1)-N(1)	2.136(4)
Cu(1)-N(3)	1.959(5)	Cu(1)-N(2)#1	2.162(4)
#1 -x-1,y-1/2,-z-1/2	#2 x+1/2,-y+1/2,-z		
#3 -x-1,y+1/2,-z-1/2	#4 x-1/2,-y+1/2,-z		

Table S6 Selected angles ($^{\circ}$) for **3**

3			
C(31)-Cu(1)-N(3)	130.91(17)	C(10)-N(1)-Cu(1)	120.1(3)
C(31)-Cu(1)-N(1)	116.78(17)	C(11)-N(1)-Cu(1)	122.8(3)
N(3)-Cu(1)-N(1)	99.91(16)	C(1)-N(2)-Cu(1)#3	120.4(3)
C(31)-Cu(1)-N(2)#1	107.10(18)	C(3)-N(2)-Cu(1)#3	122.4(3)
N(3)-Cu(1)-N(2)#1	102.63(17)	C(31)#2-N(3)-Cu(1)	178.6(4)
N(1)-Cu(1)-N(2)#1	92.14(15)		
#1 -x-1,y-1/2,-z-1/2	#2 x+1/2,-y+1/2,-z		
#3 -x-1,y+1/2,-z-1/2	#4 x-1/2,-y+1/2,-z		